Theoretical description of phase equilibrium in the nickel-titanium system

1991 J. Phys.: Condens. Matter 3 9965

(http://iopscience.iop.org/0953-8984/3/50/002)

J. Phys.: Condens. Matter 3 (1991) 9965–9974. Printed in the UK

Theoretical description of phase equilibrium in the nickel–titanium system

D H Le, C Colinet, P Hicter and A Pasturel

Laboratoire de Thermodynamique et Physico-chimie Métallurgiques, Ecole Nationale Supérieure d'Electrochimie et d'Electrométallurgie de Grenoble, BP 75, 38402 Saint Martin d'Hères Cédex, France

Received 10 June 1991, in final form 29 July 1991

Abstract. Solid–solid and solid–liquid phase equilibrium in the Ni–Ti system is studied within the framework of the cluster variation method (CVM). The energy parameters entering the free-energy description of each phase are determined by tight-binding energy calculations using the cluster Bethe lattice method (CBLM). For simplicity, the pair interactions are restricted to first-nearest neighbours in FCC-based structures and to first- and second-nearest neighbours in BCC-based structures. The configurational entropy for disordered solutions and for ordered compounds are obtained using the tetrahedron approximation of the CVM. The three compounds NiTi, Ni_3Ti and $NiTi_2$ compounds are treated as stoichiometric compounds. The calculated diagram agrees reasonably well with that determined experimentally.

1. Introduction

The possibility now exists of deriving phase diagrams from combining at a high level of accuracy both quantum mechanical and statistical thermodynamical contributions. These calculations have to take into account the local chemical environment (i.e. short-range order (SRO)) which is important in determining both the internal energy and the entropy. One of the most efficient methods for including SRO in the configurational free-energy function is the cluster variation method (CVM) [1]. In the more general problem of incoherent equilibrium, i.e. equilibrium between phases based on different crystal lattices, the CVM requires, as input, the energy of the completely disordered states for the different lattices and effective cluster interactions (ECIS) which determine ordering or clustering reactions occurring on a given lattice. In fact, these interactions must be defined carefully and depend on the approximation of the CVM. These energy terms may be obtained numerically by means of electronic structure calculations by two different procedures. The first approach is the so-called Connolly–Williams [2] method; in this approach, it is assumed that, for each lattice, the total energy can be written as a sum of configuration-independent ECIS multiplied by the multisite correlation functions. In practice it requires the existence of a maximum cluster beyond which the cluster interactions are supposed to be negligible and one performs total energy calculations of as many ordered superstructures as there are unknown cluster interactions. This procedure has been used successfully by Zunger and co-workers [3], by Terakura *et al* [4] and also by Sluiter *et al* [5]. In the second approach, the starting point is the fully disordered state,

0953-8984/91/509965 + 10 $03.50

its energy being calculated by the coherent-potential approximation (CPA) [6]. The ECIs are then calculated by the embedded-cluster method [7] or by the generalized perturbation method (GPM) [8] using a perturbative treatment about the completely disordered state. In this case, the ordering energies can be written as an expression in terms of concentration-dependent *l*th-order ECIs. GPM can be developed with the first-principles multiple-scattering formalism of the Korringa–Kohn–Rostoker CPA [9] or more simply in the framework of the tight-binding (TB) approximation [10]; an alternative approach, called the alloy cluster Bethe lattice method (CBLM) has been proposed by Robbins and Falicov [11]. This approach presents a great advantage in including SRO explicitly in the calculation of the electronic spectrum and internal energy, and in treating charge transfer in a self-consistent way. However, perhaps, the most interesting aspect of this approach is that the study of SRO can be extended to the topologically disordered systems such as amorphous or liquid materials, using a scalar approximation [12]. One can thus treat both the solid and the liquid part of the phase diagram at the same level of approximation, which is a necessary condition for studying the equilibrium between liquid and compounds or solid solutions.

In this paper, we studied the Ni–Ti phase diagram which is of both theoretical and technological importance. Around equiatomic composition, Ni–Ti alloys exhibit interesting shape memory effects and corrosion resistance. Tso and Sanchez [13] have shown that the CVM tetrahedron approximation using pairwise interactions as energy parameters determined from available thermochemical data is able to give a good representation of the phase diagram. In a previous paper [14], TB calculations of the electronic structure of NiTi compounds and their cohesive properties have been presented. Calculated ground states at zero temperature are found to be in good agreement with the experimental crystal structures observed for the three Ni_3Ti, NiTi and $NiTi_2$ compounds. To extract effective pair interactions, we have assumed that the alloy energy of formation can be written as the sum of a non-local term describing the energy of the random alloy plus an ordering term given these concentration-dependent effective pair interactions. Their manifestation on the phase diagram determination via the tetrahedron approximation of the CVM is now presented.

The paper is organized as follows: in section 2, we present a brief review of the quantum and statistical mechanical approaches used in our calculations. In section 3, a complete equilibrium phase diagram is calculated for the Ni–Ti system and compared with the experimental diagram.

2. Free-energy model

In order to compute the phase diagram, we need to know the free energy of the binary alloy in its given phase, and then its energy but also its entropy of formation. For the alloy in its phase α, the total free energy may be written as

$$F^\alpha = xF_A^\alpha + (1-x)F_B^\alpha + E_f^\alpha - TS_f^\alpha \tag{1}$$

where x is the concentration of element A, F_I^α, is the free energy of pure element I in phase α, and E_f^α and S_f^α respectively, are, the enthalpy and entropy of alloy formation.

The first simplifying assumption regarding the evaluation of this total free energy is to assume that the free energy for the pure elements can be written as

$$F_I^\alpha = E_I^\alpha - TS_I^\alpha \tag{2}$$

in which the cohesive energy E_I^α and entropy S_I^α are both considered to be temperature independent.

The second assumption is to consider that S_f^c is a purely configurational term, which means in other terms that the remaining entropy depends only on the concentration via the first two terms on the right-hand side of equation (1).

2.1. Energy of formation

As mentioned in the introduction, the energy of formation is written as the sum of a non-local energy term (associated with the random alloy) and a local ordering energy contribution:

$$E_f = E_{rand}(x) + E_{ord}(x, \sigma) \tag{3}$$

where $E_{rand}(x) = E_f(x, 0)$ is the energy of formation of the random alloys and where the ordering energy E_{ord} takes into account the contribution σ, due to short-range order [15].

E_{rand} is a function only of the point correlation function $\zeta_1 = 2x - 1$. As previously used [15], E_{rand} can be expressed by the polynomial expression.

$$E_{rand}(x) = (A_0 + B_0\zeta_1 + C_0\zeta_1^2 + D_0\zeta_1^3)(1 - \zeta_1^2). \tag{4}$$

In terms of effective pair interactions, the ordering energy is written

$$E_{ord} = \tfrac{1}{2}\sum_k z_k V_k(x)(\zeta_2^{(k)} - \zeta_1^2) \tag{5}$$

where z_k, $V_k(x)$ and $\zeta_2^{(k)}$ respectively, are, the coordination number, effective pair interaction and pair correlation function of the kth-nearest neighbour.

For transition-metal alloys, keeping pair interactions between first-nearest neighbours for FCC-based and between first- and second-nearest neighbours for BCC-based structures is a good approximation [16]. Then the ordering energy becomes

$$E_{ord}^{FCC}(x, \sigma) = [4x(1 - x)z/2]V_1(x)\sigma \tag{6a}$$

$$E_{ord}^{BCC}(x, \sigma_1, \sigma_2) = 4x(1 - x)[(z_1/2)V_1(x)\sigma_1 + (z_2/2)V_2(x)\sigma_2]. \tag{6b}$$

Given (6), the interactions are determined by calculating $E_{ord}(x, \sigma)$ as a function of the SRO parameter σ, using the TB CBLM. For the Ni–Ti system, the EPIS display a strong concentration dependence for both lattices, their large positive values being consistent with the strongly negative energies of formation found in the Ni-rich part. It has also been shown that these results are in very good agreement with those obtained from the TB GPM CPA [14].

We have then the possibility of calculating the energies of formation of solid solutions or superstructures based on the BCC and FCC lattices.

For compounds with complex structures such as the $D0_{24}$ hexagonal Ni_3Ti compound and the $E9_3$ cubic $NiTi_2$ compound, the recursion method [17] has been used to obtain the energies of formation. The coherence between the two methods of the calculation of the formation energy has been checked [14].

2.2. Configurational entropy

As for the energies of formation, different configurational entropy approximations depending on the nature of the phase being considered are used. For the strictly stoichiometric compounds, the configurational entropy is taken to be equal to zero. For

solid solutions or ordered phases presenting an extended concentration range such as the B2 phase, the configurational entropy is described by means of the CVM. The maximum cluster used in our study is the tetrahedron containing first and second neighbours in the BCC lattice; in this approximation, the molar entropy of a BCC disordered system is given by

$$S^{\mathrm{BCC}} = -R\Big(6\sum_{ijkl} w_{ijkl}\ln w_{ijkl} - 12\sum_{ijk} t_{ijk}\ln t_{ijk} + 3\sum_{ij} y_{ij}^{(2)}\ln y_{ij}^{(2)} + 4\sum_{ik} y_{ik}^{(1)}\ln y_{ik}^{(1)} - \sum_{i} x_i \ln x_i\Big) \tag{7}$$

where w_{ijkl}, t_{ijk}, $y_{ij}^{(2)}$, $y_{ik}^{(1)}$ and x_i respectively, denote, the probabilities of finding tetrahedra, triangles, second-neighbour pairs, first-neighbour pairs and points in the configuration given by their subscripts (i represents A or B in a binary alloy). R is the perfect gas constant.

For the disordered FCC structure we have

$$S^{\mathrm{FCC}} = -R\Big(2\sum_{ijkl} w_{ijkl}\ln w_{ijkl} - 6\sum_{ij} y_{ij}^{(1)}\ln y_{ij}^{(1)} + 5\sum_{i} x_i \ln x_i\Big). \tag{8}$$

The cluster probabilities are related by the following consistency relationships:

$$t_{ijk} = \sum_{l} w_{ijkl} \tag{9a}$$

$$y_{ij}^{(2)} = \sum_{kl} w_{ijkl} \tag{9b}$$

$$y_{ik}^{(1)} = \sum_{jl} w_{ijkl} \tag{9c}$$

$$x_i = \sum_{jkl} w_{ijkl}. \tag{9d}$$

For the case of an ordered phase presenting a concentration range, long-range order is described in the usual manner by means of sublattices reflecting the symmetry of the ordered structure. A given cluster may now have points in the crystal belonging to different sublattices and their probabilities have to be distinguished accordingly (see [18] for more details).

2.3. Liquid alloys

Liquid alloys may also display SRO as has been shown recently [19], and it is essential to take it into account in the determination of their thermodynamic data. To perform such calculations, a reference system characterized by a mixture of hard spheres which all have the same diameter but different charges and which interact through a screened Coulomb potential [20] is a good starting point for a variational method. This reference system has been found, coupled with pseudopotentials or TB CBLM, to describe the structural and thermodynamic manifestations of ordering in disordered alloys well [21]. If we are interested only in the thermodynamic data, similar results are found for transition-metal-based alloys if the liquid configurational free energy is approximated by the tetrahedron approximation of the CVM free energy in the disordered FCC structure but now with the first-nearest-neighbour interactions calculated within the Bethe lattice

approximation using an isotropic environment [12]. In this case the coordination number z is the relevant parameter and has been chosen to be equal to 12, a value which is consistent with the local coordination found in the liquid metallic alloys [19]. We have used this approximation to describe the Ni–Ti liquid phase in the present work.

2.4. Phase equilibrium

In order to determine the equilibrium phase diagram, it is more convenient to minimize the grand potential Ω given by

$$\Omega = F - \mu\zeta_1 \tag{10}$$

where μ is the effective chemical potential. In the present work, the minimization of the grand potential is carried out with respect to a set of independent configurational variables; in the case of the tetrahedron approximation, these configurational variables are chosen to be the tetrahedron probabilities w_{ijkl} at constant temperature T and effective chemical potential μ, taking into account the normalization constraint

$$\sum_{ijkl} w_{ijkl} = 1. \tag{11}$$

This minimization is done using the natural iteration (NI) method developed by Kikuchi [22]. The NI equations used in the present model have been presented elsewhere [23] and will not be repeated here.

The equilibrium phase diagram between two phases I and II is computed using the same scheme as that proposed by Kikuchi and De Fontaine [18]. For the same initial value of the effective chemical potential μ, the grand potential Ω_I of phase I and the grand potential Ω_{II} of phase II are calculated using the procedure described above. If $\Omega_I = \Omega_{II}$, the equilibrium conditions are realized but, if not, the value of μ is modified until $\Omega_I = \Omega_{II}$.

3. Results for the Ni–Ti system

The Ni–Ti phase diagram displayed in figure 1 is characterized by a liquid phase, a FCC (A_1) phase in the Ni-rich part, a BCC (A_2) phase in the Ti-rich part at high temperatures, two stoichiometric compounds $NiTi_2$ and Ni_3Ti and one intermediate phase NiTi with a variable range of solubility [24].

3.1. Energies of formation of compounds

As a first step, we present the values of the energies of formation of the three intermediate phases observed in the equilibrium phase diagram. As already explained in the previous section, for the two stoichiometric compounds Ni_3Ti and $NiTi_2$, we have used the tight-binding Hamiltonian described in [14] and coupled with the recursion method while, for the NiTi compound, the alloy CBLM has been chosen.

At this level of discussion it is essential to recall the main ingredients used in our TB Hamiltonian.

(i) Our calculations have been carried out by use of a self-consistent Hartree–Fock Hamiltonian with a five-orbital basis per atom (the five d orbitals). Accordingly the

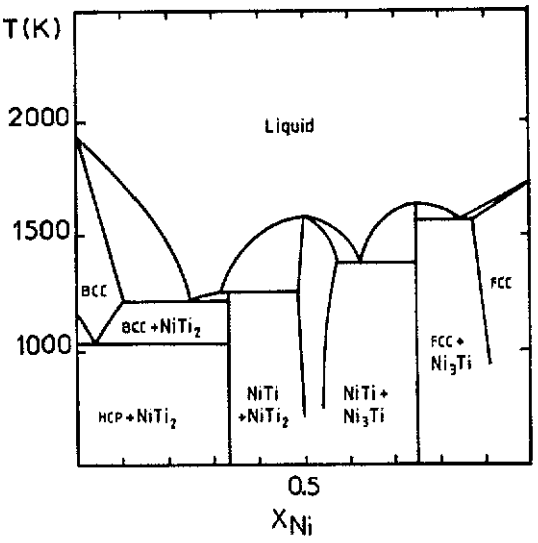

Figure 1. Experimental phase diagram of the Ni–Ti system.

effects of s and p electrons on the energies of formation are neglected; retaining the d part is sufficient to explain the strong negative values of the alloying formation energies in the Ni–Ti system.

(ii) The hopping integrals for the pure elements are determined with canonical Slater–Koster parameters according to the prescription of Harrison [25]. The Slater–Koster parameters between unlike atoms in the alloy are estimated following Shiba [26], as the geometric mean of those for the pure metals.

(iii) The on-site energy for pure metal i is taken to be equal to the d energy level in the excited-free-atom configuration $s^1d^{(v_i-1)}$, where v_i is the number of valence electrons.

(iv) As already discussed previously [14], the repulsive part of the total energy has been neglected since all the studied compounds or solid solutions are based on close-packed structures and thus have similar local environments [27].

For $x_{Ni} = 0.75$, we have checked that the $D0_{24}$ hexagonal structure is more stable than the $L1_2$ or $D0_3$ cubic structure; in a similar way, for $x_{Ni} = 0.5$, we have found that the B2 structure is more stable than the $L1_0$ or B32 structure. All the results are gathered in table 1.

3.2. Effective pair interactions and disordered alloys

Extraction of EPIs from CBLM calculations for both FCC- and BCC-based structures has been already discussed in [14] and will not be repeated here. These EPIs display a strong concentration dependence, their large positive values at the Ni-rich end being consistent with the behaviour of the Ni_3Ti compound which remains ordered up to its melting point.

Table 1. Calculated energies of formation in the Ni–Ti system. Ni FCC and Ti HCP are the reference state.

Structure	ΔH_f (kJ mol^{-1})
$NiTi_3$ ($L1_2$)	−19.3
$NiTi_3$ ($D0_3$)	−19.3
$NiTi_2$ ($E9_3$)	−35
NiTi ($L1_0$)	−40.8
NiTi (B2)	−47
NiTi (B32)	−37.1
Ni_3Ti ($L1_2$)	−44.8
Ni_3Ti ($D0_3$)	−44.6
Ni_3Ti ($D0_{24}$)	−46.4

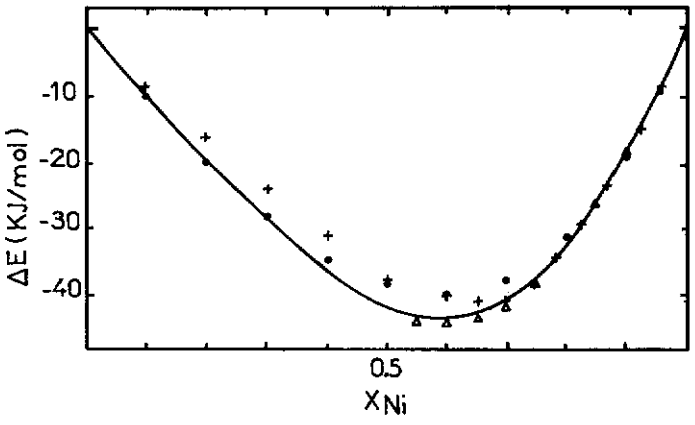

Figure 2. Internal energies for the liquid phase ($T = 1838$ K): +, from [28]; ○, data from [29]; △, data from [30].

3.3. Liquid phase

To calculate the energy of formation of the liquid phase, we have used the same TB Hamiltonian as for the solid part of the phase diagram but with a scalar version of the alloy CBLM which is a very appropriate method for describing liquid systems [12]. In figure 2 are compared our calculated values which the experimental data [28–30]; the agreement is very good, especially for the Ni-rich part. Let us mention that the evolution as a function of the composition is very similar to those of BCC- and FCC-based solid solutions.

3.4. Phase diagram

We have seen that TB Hamiltonian coupled with the CBLM or recursion method gives a good trend of the energies of formation of the different phases occurring in the Ni–Ti system. However, to obtain the phase diagram, there is still a 'missing link' in our

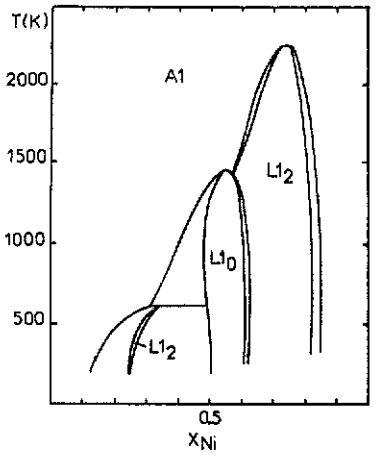

Figure 3. The FCC Ni–Ti phase diagram.

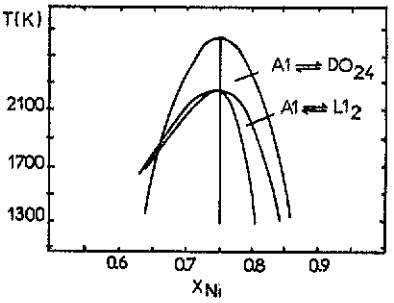

Figure 4. Stable equilibrium $Ni(A_1) \leftrightarrow Ni_3Ti$ ($D0_{24}$) and metastable equilibrium $Ni(A_1) \leftrightarrow N_3Ti$ ($L1_2$).

approach which is the thermodynamic properties of the pure metals or in other words the difference between the free energies of the liquid and crystalline phases. Although density functional theory has made significant progress in the modelling of liquids, application to the determination of the melting temperature does not yet appear possible and is beyond the scope of our TB Hamiltonian. Therefore, we have chosen to use thermodynamic compilations to obtain melting temperatures and the latent heat of melting for both Ni and Ti elements [31].

If only FCC-based equilibria are considered, the phase diagram in figure 3 is produced. Both $L1_2$ and $L1_0$ phase regions are obtained with two points of transformation: the first corresponds to the peritectoid reaction $A_1 + L1_0 \leftrightarrow L1_2$ for $T = 650$ K and the second is the eutectoid reaction $A_1 \leftrightarrow L1_0 + L1_2$ for $T = 1433$ K.

It is interesting to compare the metastable equilibrium $Ni(A_1) \leftrightarrow Ni_3Ti(L1_2)$ with the stable equilibrium $Ni(A_1) \leftrightarrow Ni_3Ti(D0_{24})$. The corresponding phase diagrams are shown in figure 4. It can be seen that, for temperatures below 1600 K and for a concentration range $0.75 < x_{Ni} < 1$, the concentrations of the A_1 phase are similar in the two equilibria, the A_1 phase in the $Ni(A_1) \leftrightarrow Ni_3Ti(D0_{24})$ equilibrium being slightly more Ni rich than the A_1 phase of the other equilibrium. In figure 5 are displayed the free-energy curves of the three A_1, $L1_2$ and $D0_{24}$ phase as a function of x_{Ni} for $T =$ 1500 K. The concentrations of the equilibrium phases are obtained by common tangent constructions; the conclusion is that it seems to be possible to obtain the metastable $L1_2$ phase from the A_1 phase if rapid cooling is used for instance.

When both FCC- and BCC-based free-energy curves are combined with the liquid free energy and with the free energies of the three compounds, the complete phase diagram in figure 6 is obtained. Although the cubic B2 phase is experimentally reported to be stable over a small concentration range, it has been described as a stoichiometric compound. At high temperatures, the NiTi phase diagram can be viewed as resulting from a BCC–FCC competition. FCC dominates on the Ni side with the FCC solid solution and the metastable $L1_2$ (Ni_3Ti) FCC superstructure. On the Ti side, BCC dominates with an important BCC Ti terminal phase above 710 K. In the Ni-rich part, the agreement with

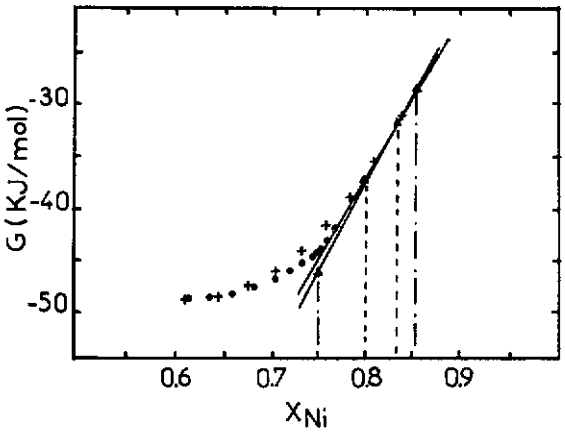

Figure 5. Free-energy curves of A_1 (+), $L1_2$ (○) and $D0_{24}$ (△) phases at $T = 1500$ K.

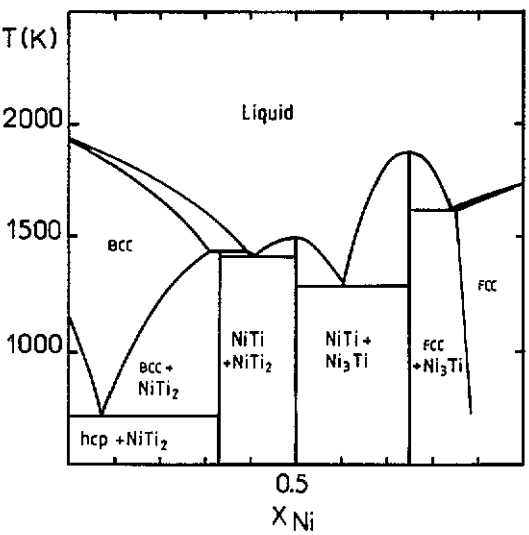

Figure 6. The calculated Ni–Ti phase diagram.

the experimental phase diagram is very good. The congruently melting temperatures of Ni_3Ti and NiTi compounds are correctly predicted like the eutectic temperature. It is imperative to recognize that there is no alloy parameter to describe the solid alloy part nor to obtain the liquid alloy curve. On the Ti-rich part, the agreement is less satisfying. The solid A2 solution seems to be too stable and therefore its stability range is too important in comparison with the experimental range. The eutectic equilibrium is found to be between NiTi and $NiTi_2$ compounds while it is between $NiTi_2$ and A2 experimentally. It is difficult to analyse the origin of the discrepancy but our calculations seem to stabilize the BCC structure too much.

The stability of the B2 phase can be understood using simple arguments similar to those used to explain the BCC–FCC competition for pure transition metals. Mixing Ni and Ti corresponds to an average number of d electrons more favourable for the BCC structure than for the FCC structure.

4. Conclusion

The TB calculation of the Ni–Ti system gives results in good agreement with experimental information. (i) We are able to predict the correct ground states especially for $x_{Ni} = 0.5$ and 0.75. The equiatomic compound crystallizes in the B2 structure which is more stable than the $L1_0$ structure and, for $x_{Ni} = 0.75$, the $D0_{24}$ structure is more stable than $L1_2$ or $D0_3$ structures. (ii) Taking into account chemical SRO to describe the free energy of the liquid phase is essential. We find a congruent melting temperature for NiTi and Ni_3Ti compounds but the phase boundaries of the peritectic decomposition of the $NiTi_2$ compound are not the same as in the experimental phase diagram; it is worth noting that this part of the phase diagram is very sensitive to the values of the energies of the three phases which determine the equilibrium properties but the BCC-based solid solution seems to be too exothermic with respect to the other phases.

References

[1] Kikuchi R 1951 *Phys. Rev.* **81** 998
[2] Connolly J W D and Williams A R 1983 *Phys. Rev.* B **27** 5169
[3] Ferreira L G, Mbaye A A and Zunger A 1987 *Phys. Rev.* B **35** 6475
Mbaye A A, Ferreira L G and Zunger A 1987 *Phys. Rev. Lett.* **58** 49
[4] Terakura K, Oguchi T, Mohri T and Watanabe K 1987 *Phys. Rev.* B **35** 2169
Mohri T, Terakura K, Oguchi T and Watanabe K 1988 *Acta Metall.* **36** 547
[5] Sluiter M, de Fontaine D, Guo X Q, Podloucky R and Freeman A J 1990 *Phys. Rev.* B **42** 10 460
[6] Velicky B, Kirkpatrick S and Ehrenreich H 1968 *Phys. Rev.* **175** 747
[7] Gonis A and Garland J W 1977 *Phys. Rev.* B **16** 2424
[8] Ducastelle F and Gautier F 1976 *J. Phys. F.: Met. Phys.* **6** 2039
[9] Turchi P E A, Stocks G M, Butler W H, Nicholson D M and Gonis A 1988 *Phys. Rev.* B **37** 5982
[10] Ducastelle F 1989 *Alloy Phase Stability* ed G M Stocks and A Gonis (Deventer: Kluwer) p 293
[11] Robbins M D and Falicov L M 1984 *Phys. Rev.* B **28** 1333
[12] Mayou D, Nguyen Manh D, Pasturel A and Cyrot-Lackmann F 1986 *Phys. Rev.* B **33** 3384
[13] Tso N C and Sanchez J M 1989 *High Temperature Ordered Alloys III (Materials Research Society Symp. Proc. 133)* (Pittsburgh, PA: Materials Research Society) p 63
[14] Le D H, Colinet C, Hicter P and Pasturel A 1991 *J. Phys.: Condens. Matter* **3** 7895
[15] Colinet C, Bessoud A and Pasturel A 1989 *J. Phys.: Condens. Matter* **1** 5837
[16] Sluiter M and Turchi P 1989 *Phys. Rev.* B **40** 11215
[17] Haydock R 1980 *Solid State Physics* vol 35, ed H Ehrenreich, D Turnbull and F Seitz (New York: Academic) p 215
[18] Kikuchi R and de Fontaine D 1978 *National Bureau of Standards Report* NOSP-496, p 967
[19] Maret M, Pomme T, Pasturel A and Chieux P 1990 *Phys. Rev.* B **42** 1598
[20] Pasturel A, Hafner J and Hicter P 1985 *Phys. Rev.* B **32** 5009
[21] Pasturel A and Hafner J 1986 *Phys. Rev.* B **34** 8357
[22] Kikuchi R 1974 *J. Chem. Phys.* **60** 1071
[23] Sigli C and Sanchez J M 1985 *Acta Metall.* **33** 1097
[24] Hansen M and Anderko K 1985 *Constitution of Binary Alloys* (New York: McGraw-Hill) pp 1049–53
[25] Harrison W A 1980 *Electronic Structure and the Properties of Solids* (San Francisco, CA: Freeman) pp 476–500
[26] Shiba H 1971 *Prog. Theor. Phys.* **46** 77
[27] Pettifor D G 1986 *J. Phys. C: Solid State Phys.* **19** 285
[28] Lück R and Arpshofen I 1988 *Thermochim. Acta* **131** 171
[29] German R M and Saint Pierre G R 1972 *Metall. Trans.* **3** 2819
[30] Esin Yu O, Valishev M G, Ermakov A F, Gel'd O V and Petrushevsku M S 1981 *Russ. J. Phys. Chem.* **55** 421
[31] Dinsdale A T 1988 SGTE data for pure elements *National Physical Laboratory Report*